

*Division of Particle and Astrophysical Science, Nagoya University
Department of Mathematics and Physics, Osaka City University*

OCU-PHYS 493
AP-GR 152
NITEP 4

Constant-mean-curvature Slicing of the Swiss-cheese Universe

Chul-Moon Yoo^{1,*} and Ken-ichi Nakao^{2,†}

¹*Division of Particle and Astrophysical Science,
Graduate School of Science, Nagoya University, Nagoya 464-8602, Japan*

²*Department of Mathematics and Physics,
Graduate School of Science, Osaka City University,
3-3-138 Sugimoto, Sumiyoshi, Osaka 558-8585, Japan*

A sequence of Constant-Mean-Curvature(CMC) slices in the Swiss-Cheese(SC) Universe is investigated. We focus on the CMC slices which smoothly connect to the homogeneous time slices in the Einstein-de Sitter region in the SC universe. It is shown that the slices do not pass through the black hole region but white hole region.

* yoo@gravity.phys.nagoya-u.ac.jp

† knakao@sci.osaka-cu.ac.jp

I. INTRODUCTION

Numerical simulations of spacetime dynamics in cosmological settings have been actively performed in recent years. One main motivation to simulate the cosmological nonlinear dynamics is to quantify the effect of the non-linear small scale inhomogeneity on the global expansion law of the universe[1–16]. Another significant motivation comes from primordial black holes[17, 18]. Spherically symmetric simulations of primordial black hole formation have been repeated in different settings[19–28]. Non-spherical simulation of gravitational collapse in an expanding background has been recently performed in Ref. [29].

When we analyze a spacetime dynamics with a numerical procedure, the dynamics is described as a sequence of time slices, that is, a foliation by a one-parameter family of spacelike hypersurfaces. Therefore, in order to understand the spacetime structure, the domain covered by the sequence of time slices should be correctly figured out. For this purpose, a sequence of time slices in a well-known analytic spacetime is often helpful. One of the useful time slice conditions is the so-called Constant-Mean-Curvature(CMC), which requires a uniform value of the trace of the extrinsic curvature of each time slice. A CMC slice is often taken as the initial hypersurface for numerical simulations because it simplifies the Hamiltonian and momentum constraint equations under certain assumptions. CMC slices in the Schwarzschild(Sch) spacetime may give a helpful insight to understand the intrinsic geometry and the embedding of the initial hypersurface for a dynamical simulation associated with black hole formation.

There are several works on CMC and other slices for well-known spacetimes(see e.g., [30–35]). In this paper, we investigate CMC slices in the Swiss-Cheese(SC) universe[36, 37]. The SC universe model is constructed by arbitrarily removing spherical regions from the Einstein-de Sitter (EdS) universe model in a non-overlapping manner, and filling each removed region with a region of the Sch spacetime whose center is occupied by a black or white hole. Thus, the SC universe is composed of the interior Sch region and exterior EdS region which are matched each other with Israel’s junction condition[38]. In the EdS region, we consider the trivial CMC slice, that is, the homogeneous slice on which the value of the trace of the extrinsic curvature is given by $3H$ with H being the Hubble constant. Therefore, what we investigate in this paper is just a sequence of CMC slices in the Sch spacetime. The difference from previous studies on CMC slices in the Sch spacetime is in the boundary condition on the boundary between the Sch and EdS regions. The previous studies on a foliation of a black hole spacetime with CMC slices are applicable to only totally spherically symmetric spacetimes. By contrast, the CMC slices in the present study will be applicable to the situations in which black holes are randomly distributed in the expanding universe. The knowledge about the CMC slices in the SC universe may be helpful to get better insight into the geometry of the initial hypersurface.

This paper is organized as follows. In Sec. II, we review the SC universe deriving the equation describing the boundary between the Sch and EdS regions. The ordinary differential equations for CMC slices with the Kruskal coordinates are derived in Sec. III, and results are shown in Sec. IV.

We use the geometrized units in which both the speed of light and Newton's gravitational constant are one. The Greek indices run from 0 to 3 and the Latin indices run from 1 to 3.

II. MATCHING EDS AND THE SCH SPACETIME

As mentioned, the SC universe model is constructed by removing spherical regions from the EdS universe model and filling each removed domain by a spherical domain of the Sch spacetime. We briefly review the SC universe model to fix the notation in this section deriving the motion of a boundary between the EdS and the Sch regions.

A. Boundary on the EdS side

The line element of the EdS spacetime can be written as

$$ds^2 = -d\tau^2 + a(\tau)^2 (d\chi^2 + \chi^2 d\Omega^2), \quad (1)$$

where $a(\tau)$ is the scale factor, and $d\Omega^2 = d\theta^2 + \sin^2\theta d\phi^2$ is the round metric. If we set $a = a_h$ at $\tau = \tau_h$, we have

$$a(\tau) = a_h \left(\frac{\tau}{\tau_h} \right)^{2/3}. \quad (2)$$

The one-parameter family of the timelike hypersurfaces with constant χ foliate the EdS spacetime. On each hypersurface of constant χ , we use the intrinsic coordinates ξ^i defined by

$$\xi^i = (\tau, \theta, \phi). \quad (3)$$

Then, the induced metric h_{ij} on a hypersurface of constant χ is given by

$$h_{ij} d\xi^i d\xi^j = -d\tau^2 + a(\tau)^2 \chi^2 d\Omega^2. \quad (4)$$

We remove a spherical region $\chi < \chi_b$ in the EdS universe model and fill it with a region of the Sch spacetime. The boundary between the Sch and the EdS regions is a timelike hypersurface Σ_0 of

$$\chi = \chi_b. \quad (5)$$

Defining $A(\tau)$ as

$$A(\tau) := a(\tau)\chi_b = A_h \left(\frac{\tau}{\tau_h} \right)^{2/3}, \quad (6)$$

we obtain the following form of the induced metric h_{ij}^b on Σ_0 :

$$h_{ij}^b d\xi^i d\xi^j = -d\tau^2 + A(\tau)^2 d\Omega^2, \quad (7)$$

where we have defined A_h by $A_h = a_h \chi_b$.

As is well known, for the Gaussian normal coordinate, the extrinsic curvature tensor k_{ij} of Σ_0 is given by

$$k_{ij} = \frac{1}{2} \ell^\mu \partial_\mu h_{ij} \big|_{\chi=\chi_b}, \quad (8)$$

where ℓ^μ is the normalized vector which is normal to Σ_0 . Since we have

$$\ell^\mu \partial_\mu = \frac{1}{a} \partial_\chi, \quad (9)$$

nonzero components of the extrinsic curvature are given by

$$k_{\theta\theta} = \frac{k_{\phi\phi}}{\sin^2 \theta} = A(\tau). \quad (10)$$

B. Boundary on the Sch side

The metric of the Sch spacetime is given by

$$ds^2 = -f(r)dt^2 + \frac{1}{f(r)}dr^2 + r^2d\Omega^2, \quad (11)$$

where

$$f(r) = 1 - \frac{2M}{r}. \quad (12)$$

The boundary between the EdS and the Sch regions, Σ_0 , is described in the Sch side in the following manner:

$$t = t(\tau), \quad r = r(\tau), \quad \theta = \theta, \quad \phi = \phi. \quad (13)$$

The induced metric is given by

$$h_{ij}^b d\xi^i d\xi^j = \left(-f(r)t'^2 + \frac{r'^2}{f(r)} \right) d\tau^2 + r^2 d\Omega^2, \quad (14)$$

where $t' = dt/d\tau$ and $r' = dr/d\tau$. From the 1st Israel Junction condition (equivalence of h_{ij}^b), we obtain

$$-ft'^2 + \frac{r'^2}{f} = -1, \quad (15)$$

$$r = A_h \left(\frac{\tau}{\tau_h} \right)^{2/3}. \quad (16)$$

Setting $x^\mu = (t, r, \theta, \phi)$ and $e_i^\mu := \partial x^\mu / \partial \xi^i$, we have the expression for the extrinsic curvature k_{ij} as

$$k_{ij} = -\ell_\mu e_i^\nu \nabla_\nu e_j^\mu. \quad (17)$$

From this expression, we obtain

$$k_{\theta\theta} = \frac{1}{2} \ell_r g^{rr} \partial_r g_{\theta\theta}. \quad (18)$$

Since

$$\ell_\mu = (-r', t', 0, 0), \quad (19)$$

we find

$$k_{\theta\theta} = t' r f(r). \quad (20)$$

In this paper, we do not allow any singular shell source on the boundary. Therefore, from the 2nd Junction condition, k_{ij} must have an identical value on each side. Then, comparing the values of $k_{\theta\theta}$, we obtain

$$t' = \frac{1}{f(r)} = \left(1 - \frac{2M}{A_h} \left(\frac{\tau_h}{\tau}\right)^{2/3}\right)^{-1}. \quad (21)$$

The other non-trivial component is $k_{\tau\tau}$:

$$k_{\tau\tau} = -\ell_\mu e_\tau^\nu \nabla_\nu e_\tau^\mu. \quad (22)$$

Equation (15) is equivalent to $g_{\mu\nu} e_\tau^\mu e_\tau^\nu = -1$ and hence we have

$$g_{\alpha\beta} e_\tau^\alpha e_\tau^\nu \nabla_\nu e_\tau^\beta = 0.$$

Furthermore, we can easily find $e_\tau^\nu \nabla_\nu e_\tau^\theta = 0 = e_\tau^\nu \nabla_\nu e_\tau^\phi$. Thus, Eq. (22) and the 2nd Junction condition on τ - τ component, $k_{\tau\tau} = 0$, lead to

$$e_\tau^\nu \nabla_\nu e_\tau^\mu = 0. \quad (23)$$

This equation is just a geodesic equation.

The r component of Eq. (23) leads to

$$r'' + \frac{1}{2} \partial_r f = 0, \quad (24)$$

where we have used Eq. (15). Using Eq. (16), we obtain

$$\frac{2}{9} A_h^3 \tau_h^{-2} = M. \quad (25)$$

This condition implies that the mass inside the sphere specified by Eq. (5) in EdS is equivalent to the mass of the Sch spacetime. Actually, we can confirm it as follows:

$$M = \rho \times \frac{4}{3} \pi A^3 = \frac{3}{8\pi} H^2 \times \frac{4}{3} \pi A^3 = \frac{2}{9} A_h^3 \tau_h^{-2}, \quad (26)$$

where ρ and $H \equiv a'/a = A'/A$ are the energy density and the Hubble constant, respectively, and we have used the Friedmann equation

$$H^2 = \frac{8}{3} \pi \rho.$$

From the t -component of the geodesic equation, we obtain

$$t'' + \frac{1}{f^2} \partial_r f r' = 0. \quad (27)$$

We can check that this condition is automatically satisfied by (21).

Let us define τ_h such that $r = 2M$ at $\tau = \tau_h$, so that the area radius r of the boundary between the EdS and the Sch regions is larger than $2M$ for $\tau > \tau_h$, whereas it is less than or equal to $2M$ for $\tau \leq \tau_h$. Then, we obtain

$$A_h = 2M = \frac{3}{2}\tau_h, \quad (28)$$

where we have used Eq. (26). Finally, we obtain

$$r = \frac{3}{2}\tau_h \left(\frac{\tau}{\tau_h} \right)^{2/3}, \quad (29)$$

$$t' = \left[1 - \left(\frac{\tau_h}{\tau} \right)^{2/3} \right]^{-1}. \quad (30)$$

The second equation can be integrated as

$$\begin{aligned} t &= \tau + 3\tau_h \left(\frac{\tau}{\tau_h} \right)^{1/3} + \frac{3}{2}\tau_h \ln \left[\frac{-1 + \left(\frac{\tau}{\tau_h} \right)^{1/3}}{1 + \left(\frac{\tau}{\tau_h} \right)^{1/3}} \right] \\ &= \tau + 3\tau_h \left(\frac{\tau}{\tau_h} \right)^{1/3} - 3\tau_h \text{Arccoth} \left[\left(\frac{\tau}{\tau_h} \right)^{1/3} \right], \end{aligned} \quad (31)$$

where we have omitted the integration constant which can be chosen freely without loss of generality because of the time translational invariance. Eventually, we have only one parameter τ_h .

C. Kruskal extension

So far, we derived every equation based on the Schwarzschild coordinate system given in Eq. (11). Since the single patch of this coordinate system covers only either the outside of the horizon $r > 2M$ or the inside of the horizon $r < 2M$, we consider an analytic extension beyond the horizon $r = 2M$. The Kruskal coordinates are well known as a coordinate system which covers the whole spacetime region. For later convenience, let us consider the Kruskal extension of the trajectory of Σ_0 in the Sch spacetime. Outside the horizon, the Kruskal coordinates and the coordinates (t, r) are related as

$$T = \frac{1}{2} \left(\exp \left[\frac{t + r + r_g \ln [(r - r_g)/r_g]}{2r_g} \right] - \exp \left[\frac{-t + r + r_g \ln [(r - r_g)/r_g]}{2r_g} \right] \right), \quad (32)$$

$$R = \frac{1}{2} \left(\exp \left[\frac{t + r + r_g \ln [(r - r_g)/r_g]}{2r_g} \right] + \exp \left[\frac{-t + r + r_g \ln [(r - r_g)/r_g]}{2r_g} \right] \right). \quad (33)$$

Substituting Eqs. (29) and (31) into these expressions, we get

$$T_b(\tau) = \exp \left[\frac{1}{2} \left(\frac{\tau}{\tau_h} \right)^{2/3} \right] \left\{ \left(\frac{\tau}{\tau_h} \right)^{1/3} \sinh \left[\left(\frac{\tau}{\tau_h} \right)^{1/3} + \frac{\tau}{3\tau_h} \right] - \cosh \left[\left(\frac{\tau}{\tau_h} \right)^{1/3} + \frac{\tau}{3\tau_h} \right] \right\}, \quad (34)$$

$$R_b(\tau) = \exp \left[\frac{1}{2} \left(\frac{\tau}{\tau_h} \right)^{2/3} \right] \left\{ \left(\frac{\tau}{\tau_h} \right)^{1/3} \cosh \left[\left(\frac{\tau}{\tau_h} \right)^{1/3} + \frac{\tau}{3\tau_h} \right] - \sinh \left[\left(\frac{\tau}{\tau_h} \right)^{1/3} + \frac{\tau}{3\tau_h} \right] \right\}. \quad (35)$$

We note that the calculations in Sec. IIB can be also applied to the region $r < 2M$ and we obtain the same expression Eq. (31) for the trajectory. Therefore, the expressions (34) and (35) can be analytically extended to the region $\tau < \tau_h$.

As is clear from Eq. (6), the area radius $A(\tau)$ vanishes at $\tau = 0$ and diverges for $\tau \rightarrow \infty$. Such a timelike trajectory is possible in Sch spacetime only for the case starting from the past singularity and going to the future timelike infinity. Therefore, the boundary trajectory necessarily passes through the white hole horizon (see Fig. 1 in Sec. IV).

III. DIFFERENTIAL EQUATIONS FOR CMC SLICES

We are interested in CMC slices, that is, spacelike hypersurfaces with constant K in the SC universe, where K is the trace of the extrinsic curvature of the spacelike hypersurface. In the EdS region, we choose homogeneous time slices. Then, we extend these time slices to the Sch region keeping $K = \text{const}$. For this purpose, we derive the differential equations for CMC slices in the Sch spacetime.

We use the Kruskal coordinate system, in which the line element is written as

$$ds^2 = \frac{4r_g^3}{r(T, R)} \exp \left(-\frac{r(T, R)}{r_g} \right) (-dT^2 + dR^2) + r(T, R)^2 d\Omega^2, \quad (36)$$

where $r(T, R)$ is defined by

$$T^2 - R^2 = - \left(\frac{r - r_g}{r_g} \right) \exp \left(\frac{r}{r_g} \right). \quad (37)$$

We consider a spacelike hypersurface Σ_1 specified by the following parametric equation:

$$T = f_T(v), \quad (38)$$

$$R = f_R(v). \quad (39)$$

Covariant components of the vector normal to this surface is given by

$$N_\mu = \pm \left(-\dot{f}_R, \dot{f}_T, 0, 0 \right), \quad (40)$$

where we have chosen \pm such that N^μ is future directed, i.e., $+$ for $\dot{f}_R > 0$ and $-$ for $\dot{f}_R < 0$. The dot “ $\dot{}$ ” denotes d/dv . The contravariant components are given by

$$N^\mu = \pm \frac{r}{4r_g^3} \exp \left(\frac{r}{r_g} \right) \left(\dot{f}_R, \dot{f}_T, 0, 0 \right). \quad (41)$$

The norm is calculated as

$$N_\mu N^\mu = \frac{r}{4r_g^3} \exp\left(\frac{r}{r_g}\right) \left(-\dot{f}_R^2 + \dot{f}_T^2\right). \quad (42)$$

Using the freedom to rescale the parameter v , we can set

$$N_\mu N^\mu = - \left[\frac{r}{4r_g^3} \exp\left(\frac{r}{r_g}\right) \right]^2. \quad (43)$$

Then, the normalized vector which is normal to Σ_1 is given by

$$n^\mu = \pm \left(\dot{f}_R, \dot{f}_T, 0, 0 \right). \quad (44)$$

We note that the following equation is satisfied:

$$-\dot{f}_R^2 + \dot{f}_T^2 = -\frac{r}{4r_g^3} \exp\left(\frac{r}{r_g}\right). \quad (45)$$

Due to Eq. (45), the intrinsic metric of a CMC hypersurface is written in the form

$$d\ell^2 = dv^2 + r(f_T(v), f_R(v))^2 d\Omega^2. \quad (46)$$

This equation implies that the parameter v is the proper length measured in the radial direction, and hence we may call it the proper radial coordinate. See Appendix A for the metric of the spacetime in the CMC coordinate system.

For later convenience, we differentiate Eq. (45) with respect to R or T to obtain

$$-\dot{f}_R \partial_R \dot{f}_R + \dot{f}_T \partial_R \dot{f}_T = -\frac{\partial_R r}{8r_g^3} \exp\left(\frac{r}{r_g}\right) \left(1 + \frac{r}{r_g}\right), \quad (47)$$

$$-\dot{f}_R \partial_T \dot{f}_R + \dot{f}_T \partial_T \dot{f}_T = -\frac{\partial_T r}{8r_g^3} \exp\left(\frac{r}{r_g}\right) \left(1 + \frac{r}{r_g}\right), \quad (48)$$

where \dot{f}_T and \dot{f}_R are treated as fields on the T - R plane.

The basic equation is given by

$$K = \nabla_\mu n^\mu = 3H = \text{spatially constant}. \quad (49)$$

This equation leads to

$$\pm \frac{1}{r} \exp\left(\frac{r}{r_g}\right) \left\{ \partial_T \left[r \exp\left(-\frac{r}{r_g}\right) \dot{f}_R \right] + \partial_R \left[r \exp\left(-\frac{r}{r_g}\right) \dot{f}_T \right] \right\} = 3H. \quad (50)$$

Using

$$\ddot{f}_R = \dot{f}_R \partial_R \dot{f}_R + \dot{f}_T \partial_T \dot{f}_R,$$

we obtain

$$\partial_T \dot{f}_R = \frac{1}{\dot{f}_T} \left(\ddot{f}_R - \dot{f}_R \partial_R \dot{f}_R \right),$$

and hence, we can rewrite $\partial_T \dot{f}_R + \partial_R \dot{f}_T$ as

$$\begin{aligned}\partial_T \dot{f}_R + \partial_R \dot{f}_T &= \frac{\ddot{f}_R}{\dot{f}_T} + \frac{1}{\dot{f}_T} \left(-\dot{f}_R \partial_R \dot{f}_R + \dot{f}_T \partial_R \dot{f}_T \right) \\ &= \frac{\ddot{f}_R}{\dot{f}_T} - \frac{\partial_R r}{8 \dot{f}_T r_g^3} \exp\left(\frac{r}{r_g}\right) \left(1 + \frac{r}{r_g}\right).\end{aligned}\quad (51)$$

By a similar procedure, we obtain

$$\partial_R \dot{f}_T = \frac{1}{\dot{f}_R} \left(\ddot{f}_T - \dot{f}_T \partial_T \dot{f}_T \right)$$

and hence, we have

$$\begin{aligned}\partial_T \dot{f}_R + \partial_R \dot{f}_T &= \frac{\ddot{f}_T}{\dot{f}_R} - \frac{1}{\dot{f}_R} \left(\dot{f}_T \partial_T \dot{f}_T - \dot{f}_R \partial_T \dot{f}_R \right) \\ &= \frac{\ddot{f}_T}{\dot{f}_R} + \frac{\partial_T r}{8 \dot{f}_R r_g^3} \exp\left(\frac{r}{r_g}\right) \left(1 + \frac{r}{r_g}\right).\end{aligned}\quad (52)$$

From Eqs. (50) and (51), we obtain

$$\ddot{f}_R = \dot{f}_T \left[\pm K - \left(\frac{1}{r} - \frac{1}{r_g} \right) \left(\partial_T r \dot{f}_R + \partial_R r \dot{f}_T \right) \right] + \frac{\partial_R r}{8 r_g^3} \exp\left(\frac{r}{r_g}\right) \left(1 + \frac{r}{r_g}\right). \quad (53)$$

Similarly, from Eqs. (50) and (52), we obtain

$$\ddot{f}_T = \dot{f}_R \left[\pm K - \left(\frac{1}{r} - \frac{1}{r_g} \right) \left(\partial_T r \dot{f}_R + \partial_R r \dot{f}_T \right) \right] - \frac{\partial_T r}{8 r_g^3} \exp\left(\frac{r}{r_g}\right) \left(1 + \frac{r}{r_g}\right). \quad (54)$$

We solve these two equations with a constraint equation (45).

To solve these equations, we need explicit expressions for $\partial_T r$, $\partial_R r$ and r . Differentiating Eq.(37), we obtain

$$\partial_T r = \frac{T}{2 r_g \left(-\dot{f}_R^2 + \dot{f}_T^2 \right)}, \quad (55)$$

$$\partial_R r = \frac{-R}{2 r_g \left(-\dot{f}_R^2 + \dot{f}_T^2 \right)}. \quad (56)$$

Combining Eqs. (37) and (45), we find

$$r = r_g \ln \left[T^2 - R^2 - 4 r_g^2 \left(-\dot{f}_R^2 + \dot{f}_T^2 \right) \right]. \quad (57)$$

This final expression for r is much more convenient than Eq.(37) in our numerical integration.

IV. CMC SLICES IN THE SC UNIVERSE

A. Boundary conditions

The cosmic time τ and the areal radius r on the sphere $\Sigma_0 \cap \Sigma_1$ are denoted by τ_b and r_b , respectively. Then, the Hubble constant on $\Sigma_0 \cap \Sigma_1$ is given by

$$H = \frac{a'}{a} = \frac{2}{3\tau_b} \quad (58)$$

and, from Eq. (29), we have

$$r_b = \frac{3}{2}\tau_b \left(\frac{\tau_b}{\tau_h} \right)^{2/3} = \frac{3}{2}\tau_b \left(\frac{2}{3\tau_h H} \right)^{2/3}. \quad (59)$$

As mentioned in Sec. I, we assume that the CMC hypersurface Σ_2 in the EdS region agrees with $\tau = \tau_b$, and hence ℓ^μ is tangent to Σ_2 in the EdS side on $\Sigma_1 \cap \Sigma_2$. Since the tangent space is continuous at $\Sigma_1 \cap \Sigma_2$, ℓ^μ is also tangent to Σ_2 on the Sch side. Since we have $e_\tau^\mu \propto (T'_b, R'_b, 0, 0)$ in the Sch side, the relation $e_\tau^\mu \ell_\mu = 0$ leads to

$$\ell^\mu = C (R'_b, T'_b, 0, 0),$$

where

$$C = \sqrt{\frac{r \exp[r/r_g]}{4r_g^3 (T_b'^2 - R_b'^2)}}. \quad (60)$$

Thus, we have

$$(\dot{f}_T, \dot{f}_R, 0, 0) = -C(R'_b, T'_b, 0, 0) \quad (61)$$

on $\Sigma_1 \cap \Sigma_2$, where the negative sign has been assigned, so that the value of v increases inward.

From Eqs. (34) and (35), we obtain

$$T'_b(\tau) = \frac{1}{3\tau_h} \left(\frac{\tau}{\tau_h} \right)^{1/3} \exp \left[\frac{1}{2} \left(\frac{\tau}{\tau_h} \right)^{2/3} \right] \cosh \left[\left(\frac{\tau}{\tau_h} \right)^{1/3} + \frac{\tau}{3\tau_h} \right], \quad (62)$$

$$R'_b(\tau) = \frac{1}{3\tau_h} \left(\frac{\tau}{\tau_h} \right)^{1/3} \exp \left[\frac{1}{2} \left(\frac{\tau}{\tau_h} \right)^{2/3} \right] \sinh \left[\left(\frac{\tau}{\tau_h} \right)^{1/3} + \frac{\tau}{3\tau_h} \right]. \quad (63)$$

By using these equations, Eq. (61) gives \dot{f}_T and \dot{f}_R on $\Sigma_1 \cap \Sigma_2$ as $\dot{f}_T = -CR'_b(\tau_b)$ and $\dot{f}_R = -CT'_b(\tau_b)$, while the values of f_T and f_R on $\Sigma_1 \cap \Sigma_2$ are given as $f_T = T_b(\tau_b)$ and $f_R = R_b(\tau_b)$ with Eqs. (34) and (35). Then, we can integrate Eqs. (53) and (54) to find a CMC slice.

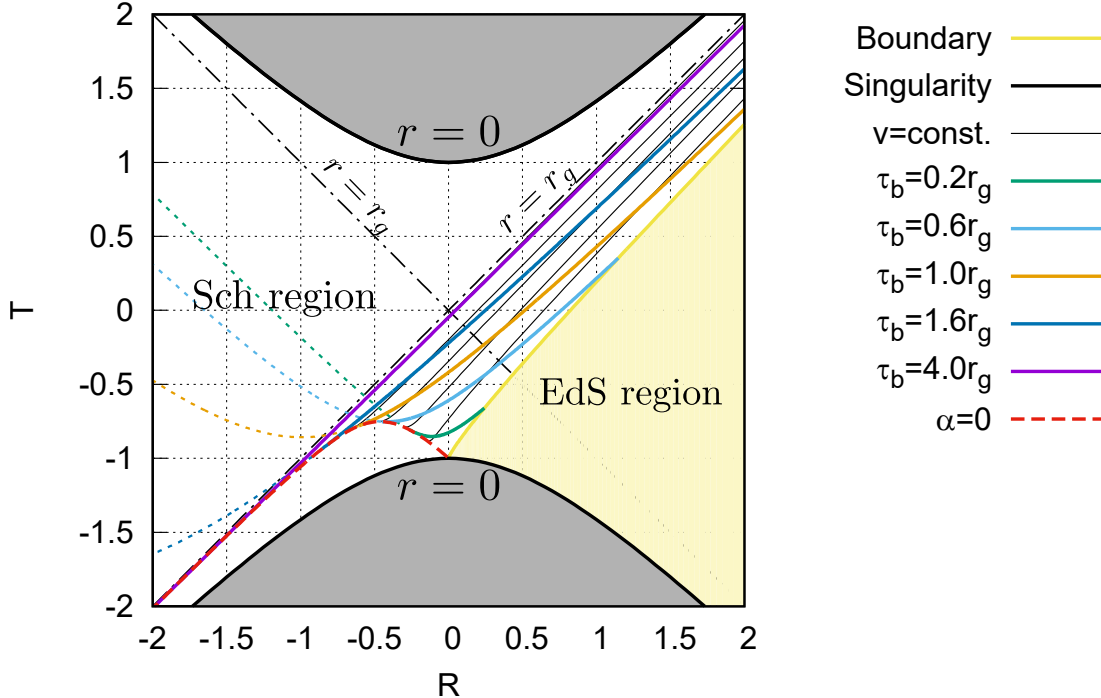


FIG. 1. CMC slices in the Sch region with the Kruskal coordinate. Each CMC slice is described by the union of a solid line segment and a dotted line segment separated by the $\alpha = 0$ point on it: α is positive on the solid segment, whereas α is negative on the dotted segment.

B. CMC slices in the Kruskal diagram

Performing numerical integrations, we finally obtain the results shown in Fig. 1. It is found from this figure that CMC slices do not pass through the black hole region but the white hole region. A similar slice is observed in an analysis of massless scalar field collapse in an expanding background[29]. In order to understand the spacetime structure of a numerical solution, one useful way is to find marginally trapped surfaces associate with the outgoing or ingoing null vector fields. To find the marginally trapped surfaces on each spacelike hyper-surface, a well studied example similar to the numerical solution often plays a crucial role. Actually, in Ref. [29], one of the present authors and his collaborators have revealed the spacetime structure by virtue of the results given in this paper. This is an example showing that the knowledge about the sequence of CMC slices obtained in this paper helps in understanding the spacetime structure of the numerical spacetime solution.

We note that, if we impose the reflection boundary condition at the center of the wormhole bridge as is in Refs. [30–33] differently from our present case, a CMC slice can pass through the black hole region. We also note that the sign of K is fixed by the boundary condition: the slice is smoothly connected to the homogeneous slice in EdS where the value of K is given by $K = -3H < 0$. If we invert the time evolution, that is, considering the collapsing

SC model, the slices do not pass through the white hole region but the black hole region (see Fig. 1 flipped upside down).

Fig. 1 shows that the CMC hypersurfaces intersect with each other. This fact implies that the lapse function α associated with the foliation by CMC hypersurfaces has zero points (see Appendix A for details). In Appendix A, we derive the following necessary and sufficient condition for the appearance of a zero point of α :

$$\mathcal{C} := \dot{f}_R \partial_\tau T - \dot{f}_T \partial_\tau R = 0, \quad (64)$$

where the coordinate system has been set as (τ, v, θ, ϕ) with $\tau = 2K$. The τ derivatives $\partial_\tau T$ and $\partial_\tau R$ can be numerically calculated by getting a nearby CMC hypersurface specified by a slightly different value of τ . From the results, we plot the curve $T = C(R)$ on which α vanishes in Fig. 1. We also plot the curves on which v is constant. In Fig. 1, each CMC slice is described by a union of solid segment and dotted segment separated by the $\alpha = 0$ point on it. It can be found that there is no intersection between the solid segments and also no intersection between the dotted segments.

The value of α can be expressed as a function of τ and v as $\alpha(\tau, v)$. Let $v_C(\tau)$ denote the value of v at which α vanishes, that is, $\alpha(\tau, v_C(\tau)) = 0$. The curve specified by $T = C(R)$ and $v = v_C(\tau)$ are equivalent to each other. Then, CMC time slicing is future directed in the domain $v < v_C(\tau)$ which is sliced by the solid segments in Fig. 1, whereas it is past directed in the domain $v > v_C(\tau)$ sliced by the dotted segments. The CMC coordinate system (τ, v, θ, ϕ) covers only the domain of $v < v_C(\tau)$ and $\tau > 0$, or equivalently $T < R$ and $T > C(R)$, i.e., the outside the black hole. The black hole region cannot be described by the foliation with the CMC slices which are smoothly connected to the homogeneous slices in EdS region.

ACKNOWLEDGEMENTS

This work was supported by JSPS KAKENHI Grant Number JP16K17688 (C.Y.).

Appendix A: Zero points of the lapse function

A CMC hypersurface is specified by the trace of the extrinsic curvature $K = 2/\tau$, or equivalently, τ , and a point on the CMC hypersurface is specified by the proper radial coordinate v and round coordinates, θ and ϕ . We refer to the coordinate system (τ, v, θ, ϕ) as the CMC coordinate system in this paper. Then, we have

$$\begin{aligned} g_{\tau\tau} &= (\partial_\tau T)^2 g_{TT} + (\partial_\tau R)^2 g_{RR} = [- (\partial_\tau T)^2 + (\partial_\tau R)^2] \Psi, \\ g_{\tau v} &= \left(-\dot{T} \partial_\tau T + \dot{R} \partial_\tau R \right) \Psi, \\ g_{vv} &= \left(-\dot{T}^2 + \dot{R}^2 \right) \Psi = 1, \end{aligned}$$

where

$$\Psi = \frac{4r_g^3}{r} \exp\left(-\frac{r}{r_g}\right),$$

a dot represents the derivative with respect to v with τ fixed, and we have used Eq. (45) in the last equality of the third equation. The spatial metric γ_{ij} , its inverse γ^{ij} and the shift vector β_i in the CMC coordinate system are

$$\begin{aligned}\gamma_{ij} &= \text{diag}\left[1, r^2, r^2 \sin^2 \theta\right], \\ \gamma^{ij} &= \text{diag}\left[1, \frac{1}{r^2}, \frac{1}{r^2 \sin^2 \theta}\right], \\ \beta_i &= (g_{\tau v}, 0, 0),\end{aligned}$$

respectively, and hence we have $\beta^i \beta_i = (g_{\tau v})^2$. From $g_{\tau\tau} = -\alpha^2 + \beta^i \beta_i$, we obtain

$$\alpha^2 = -g_{\tau\tau} + (g_{\tau v})^2 = \Psi^2 \left(\dot{R} \partial_\tau T - \dot{T} \partial_\tau R \right)^2,$$

where we have used Eq. (45). The zero point of α appears if and only if

$$\dot{R} \partial_\tau T - \dot{T} \partial_\tau R = 0 \tag{A1}$$

holds. This equation implies that the zero point of α appears if and only if the normal vector to the CMC hypersurface is orthogonal to the time coordinate basis $\partial/\partial\tau$.

-
- [1] R. W. Lindquist and J. A. Wheeler, Rev. Mod. Phys. **29**, 432 (1957), *Dynamics of a Lattice Universe by the Schwarzschild-Cell Method*.
 - [2] T. Clifton and P. G. Ferreira, Phys.Rev. **D80**, 103503 (2009), arXiv:0907.4109, *Archipelagian Cosmology: Dynamics and Observables in a Universe with Discretized Matter Content*.
 - [3] T. Clifton, K. Rosquist, and R. Tavakol, (2012), arXiv:1203.6478, *An exact quantification of backreaction in relativistic cosmology*.
 - [4] E. Bentivegna and M. Korzynski, Class.Quant.Grav. **29**, 165007 (2012), arXiv:1204.3568, *Evolution of a periodic eight-black-hole lattice in numerical relativity*.
 - [5] C.-M. Yoo, H. Abe, K.-i. Nakao, and Y. Takamori, Phys.Rev. **D86**, 044027 (2012), arXiv:1204.2411, *Black Hole Universe: Construction and Analysis of Initial Data*.
 - [6] J.-P. Bruneton and J. Larena, Class.Quant.Grav. **29**, 155001 (2012), arXiv:1204.3433, *Dynamics of a lattice Universe: The dust approximation in cosmology*.
 - [7] J.-P. Bruneton and J. Larena, Class.Quant.Grav. **30**, 025002 (2013), arXiv:1208.1411, *Observables in a lattice Universe*.
 - [8] E. Bentivegna, Class. Quant. Grav. **31**, 035004 (2014), arXiv:1305.5576, *Solving the Einstein constraints in periodic spaces with a multigrid approach*.
 - [9] C.-M. Yoo, H. Okawa, and K.-i. Nakao, Phys.Rev.Lett. **111**, 161102 (2013), arXiv:1306.1389, *Black Hole Universe: Time Evolution*.

- [10] E. Bentivegna and M. Korzynski, *Class. Quant. Grav.* **30**, 235008 (2013), arXiv:1306.4055, *Evolution of a family of expanding cubic black-hole lattices in numerical relativity.*
- [11] T. Clifton, D. Gregoris, K. Rosquist, and R. Tavakol, *JCAP* **1311**, 010 (2013), arXiv:1309.2876, *Exact Evolution of Discrete Relativistic Cosmological Models.*
- [12] M. Korzyński, (2013), arXiv:1312.0494, *Backreaction and continuum limit in a closed universe filled with black holes.*
- [13] T. Clifton, D. Gregoris, and K. Rosquist, (2014), arXiv:1402.3201, *Piecewise Silence in Discrete Cosmological Models.*
- [14] C.-M. Yoo and H. Okawa, *Phys. Rev.* **D89**, 123502 (2014), arXiv:1404.1435, *Black hole universe with a cosmological constant.*
- [15] T. Ikeda, C.-M. Yoo, and Y. Nambu, *Phys. Rev.* **D92**, 044041 (2015), arXiv:1505.02959, *Expanding universe with nonlinear gravitational waves.*
- [16] E. Bentivegna, M. Korzynski, I. Hinder, and D. Gerlicher, *JCAP* **1703**, 014 (2017), arXiv:1611.09275, *Light propagation through black-hole lattices.*
- [17] Y. B. Zel'dovich and I. D. Novikov, *Soviet Ast.* **10**, 602 (1967), *The Hypothesis of Cores Retarded during Expansion and the Hot Cosmological Model.*
- [18] S. Hawking, *Mon. Not. Roy. Astron. Soc.* **152**, 75 (1971), *Gravitationally collapsed objects of very low mass.*
- [19] D. K. Nadezhin, I. D. Novikov, and A. G. Polnarev, *Soviet Ast.* **22**, 129 (1978), *The hydrodynamics of primordial black hole formation.*
- [20] I. D. Novikov and A. G. Polnarev, *Soviet Ast.* **24**, 147 (1980), *The Hydrodynamics of Primordial Black Hole Formation - Dependence on the Equation of State.*
- [21] M. Shibata and M. Sasaki, *Phys. Rev.* **D60**, 084002 (1999), arXiv:gr-qc/9905064, *Black hole formation in the Friedmann universe: Formulation and computation in numerical relativity.*
- [22] J. C. Niemeyer and K. Jedamzik, *Phys. Rev.* **D59**, 124013 (1999), arXiv:astro-ph/9901292, *Dynamics of primordial black hole formation.*
- [23] I. Musco, J. C. Miller, and L. Rezzolla, *Class. Quant. Grav.* **22**, 1405 (2005), arXiv:gr-qc/0412063, *Computations of primordial black hole formation.*
- [24] A. G. Polnarev and I. Musco, *Class. Quant. Grav.* **24**, 1405 (2007), arXiv:gr-qc/0605122, *Curvature profiles as initial conditions for primordial black hole formation.*
- [25] I. Musco and J. C. Miller, *Class. Quant. Grav.* **30**, 145009 (2013), arXiv:1201.2379, *Primordial black hole formation in the early universe: critical behaviour and self-similarity.*
- [26] A. G. Polnarev, T. Nakama, and J. Yokoyama, *JCAP* **1209**, 027 (2012), arXiv:1204.6601, *Self-consistent initial conditions for primordial black hole formation.*
- [27] T. Nakama, T. Harada, A. G. Polnarev, and J. Yokoyama, *JCAP* **1401**, 037 (2014), arXiv:1310.3007, *Identifying the most crucial parameters of the initial curvature profile for primordial black hole formation.*
- [28] T. Nakama, *JCAP* **1410**, 040 (2014), arXiv:1408.0955, *The double formation of primordial black holes.*
- [29] C.-M. Yoo, T. Ikeda, and H. Okawa, (2018), arXiv:1811.00762, *Gravitational Collapse of a Massless Scalar Field in a Periodic Box.*
- [30] F. Estabrook *et al.*, *Phys. Rev.* **D7**, 2814 (1973), *Maximally slicing a black hole.*

- [31] K.-I. Nakao, K.-I. Maeda, T. Nakamura, and K.-I. Oohara, Phys.Rev. **D44**, 1326 (1991), *The constant mean curvature slicing of the Schwarzschild-de Sitter space-time.*
- [32] R. Beig and J. M. Heinzle, Commun.Math.Phys. **260**, 673 (2005), arXiv:gr-qc/0501020, *CMS-slicings of Kottler-Schwarzschild-de Sitter cosmologies.*
- [33] K.-i. Nakao, H. Abe, H. Yoshino, and M. Shibata, Phys. Rev. **D80**, 084028 (2009), arXiv:0908.0799, *Maximal slicing of D-dimensional spherically-symmetric vacuum spacetime.*
- [34] K. A. Dennison, T. W. Baumgarte, and P. J. Montero, Phys. Rev. Lett. **113**, 261101 (2014), arXiv:1409.1887, *Trumpet Slices in Kerr Spacetimes.*
- [35] K. A. Dennison and T. W. Baumgarte, Phys. Rev. **D96**, 124014 (2017), arXiv:1710.07373, *Schwarzschild-de Sitter spacetimes, McVittie coordinates, and trumpet geometries.*
- [36] A. Einstein and E. G. Straus, Rev.Mod.Phys. **17**, 120 (1945), *The influence of the expansion of space on the gravitation fields surrounding the individual stars.*
- [37] A. Einstein and E. Straus, Rev.Mod.Phys. **18**, 148 (1946), *Corrections and Additional Remarks to our Paper: The Influence of the Expansion of Space on the Gravitation Fields Surrounding the Individual Stars.*
- [38] W. Israel, Nuovo Cim. **B44S10**, 1 (1966), *Singular hypersurfaces and thin shells in general relativity.*